



**NTNU – Trondheim**  
Norwegian University of  
Science and Technology

# Investigation of Pressure Release Systems for CO<sub>2</sub>

**Bjørn Danielsen Ekeberg**

Master of Energy and Environmental Engineering

Submission date: February 2015

Supervisor: Petter Nekså, EPT

Co-supervisor: Håvard Rekstad, EPT  
Hans T. Haukås, EPT

Norwegian University of Science and Technology  
Department of Energy and Process Engineering



EPT-M-2014-154

**MASTER THESIS**

for

**Bjørn Ekeberg**

Autumn 2014

**Investigation of pressure release systems for CO<sub>2</sub>***Undersøkelse av trykkavlastningssystemer for CO<sub>2</sub>***Background and objective**

Closed circuits with larger amounts of CO<sub>2</sub> are becoming more and more common in industry. Examples are use as refrigerant in different refrigeration systems and transport systems for CO<sub>2</sub> for sequestration or for use in enhanced oil recovery applications.

These systems will have to handle a possible situation where the systems has to be vented, e.g. in an emergency situation or due to maintenance. This venting will most often be to the atmosphere at 1 bara, while the systems initially are at pressures ranging from 40 - 120 bara. At atmospheric pressure dry ice in equilibrium with CO<sub>2</sub> gas will be formed. This may introduce challenges and possible hazardous situations in blockage of the pressure relief valves or downstream pipe networks.

The aim of this Master's project is to perform theoretical, experimental and modelling and simulation efforts in order to better understand possible hazards for pressure release concepts proposed in the industry.

**The following tasks are to be considered:**

1. Perform a literature study related to possible hazards from the formation of dry ice during depressurisation of CO<sub>2</sub> with special emphasis on pressure relief systems.
2. Describe different pressure relief system designs applied by the (refrigeration) industry and possible measures taken to minimise adverse effects from dry ice accumulation
3. Perform an analysis of pressure development through the different pressure relief systems.
4. Plan and set up a test program for investigation and evaluation of the function of pressure relief valves and downstream pipe systems under operating conditions typical for CO<sub>2</sub> systems in supermarket refrigeration
5. Project a test setup to perform experiments simulating practical pressure relief situations, e.g. periods of long standstill, abnormal external heating, e.g. fire, and excessive discharge pressure. Perform experiments to the extent experimental infrastructure becomes available.

6. Discuss the results thoroughly from a safety point of view, and in particular in relation to the requirements in relevant standards, e.g. NS-EN 13136. If relevant, propose measures to minimise dry ice accumulation and any adverse effect from it on system functioning.

-- " --

Within 14 days of receiving the written text on the master thesis, the candidate shall submit a research plan for his project to the department.

When the thesis is evaluated, emphasis is put on processing of the results, and that they are presented in tabular and/or graphic form in a clear manner, and that they are analyzed carefully.

The thesis should be formulated as a research report with summary both in English and Norwegian, conclusion, literature references, table of contents etc. During the preparation of the text, the candidate should make an effort to produce a well-structured and easily readable report. In order to ease the evaluation of the thesis, it is important that the cross-references are correct. In the making of the report, strong emphasis should be placed on both a thorough discussion of the results and an orderly presentation.

The candidate is requested to initiate and keep close contact with his/her academic supervisor(s) throughout the working period. The candidate must follow the rules and regulations of NTNU as well as passive directions given by the Department of Energy and Process Engineering.

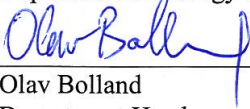
Risk assessment of the candidate's work shall be carried out according to the department's procedures. The risk assessment must be documented and included as part of the final report. Events related to the candidate's work adversely affecting the health, safety or security, must be documented and included as part of the final report. If the documentation on risk assessment represents a large number of pages, the full version is to be submitted electronically to the supervisor and an excerpt is included in the report.

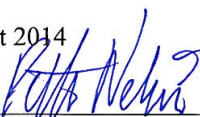
Pursuant to "Regulations concerning the supplementary provisions to the technology study program/Master of Science" at NTNU §20, the Department reserves the permission to utilize all the results and data for teaching and research purposes as well as in future publications.

The final report is to be submitted digitally in DAIM. An executive summary of the thesis including title, student's name, supervisor's name, year, department name, and NTNU's logo and name, shall be submitted to the department as a separate pdf file. Based on an agreement with the supervisor, the final report and other material and documents may be given to the supervisor in digital format.

- Work to be done in lab (Water power lab, Fluids engineering lab, Thermal engineering lab)  
 Field work

Department of Energy and Process Engineering, 20. August 2014

  
Olav Bolland  
Department Head

  
Adjunct Prof. Petter Neksa  
Academic Supervisor

Research Advisors:

Hans T. Haukås, HANS T. HAUKÅS AS

Geir A. Owren, STATOIL ASA

Håvard Rekstad, NTNU EPT

Armin Hafner, SINTEF Energy Research

# Abstract

A pressure release system for CO<sub>2</sub> is designed to release CO<sub>2</sub> from a system where the pressure is higher than a predetermined maximum pressure. Precautions has to be taken when designing a pressure release system for CO<sub>2</sub> to avoid formation of solid CO<sub>2</sub> and blockage of the safety valve and downstream pipe.

A downstream pipe simulation model was developed in order evaluate the pressure development through a downstream pipe of a pressure release system. With emphasis on supermarket refrigeration a downstream pipe geometry based on a system used in the industry was implemented in the model. The simulation model is based on the Martinelli-Nelson two-phase pressure drop equation. The calculation method was validated by comparing with former experimental study with same mass flux and geometry. Heat transfer from the ambient was also considered in the model.

The results from the simulation was compared with the standard NS-EN 13136, "Refrigerating systems and heat pumps - Pressure relief devices and their associated piping - Methods for calculation".

The simulation results showed that the low temperature at atmospheric pressure and the formation of dry ice when reaching the triple point was as expected according to theoretical calculations. For mass fluxes of 100-200 kg/sm<sup>2</sup> the triple point was reached in the last part of the downstream pipe. For mass fluxes lower than 45 kg/sm<sup>2</sup> the triple point was reached in the safety valve.

There was a significant increase in the velocity towards the end of the downstream pipe due to a decrease in density. For heat loads above 36 kW ( $G=200$  kg/sm<sup>2</sup>) and downstream diameter of 40 mm the outlet velocity became sonic ( $Ma>0.3$ ).

The pressure loss in a downstream pipe increases with increasing mass flux. The outlet flow velocity also increases with increasing mass flux. In order to avoid dry ice formation in the safety valve and to have an efficient pressure release process the mass flux should be as high as possible but without giving sonic flow velocity at the outlet.



# Sammendrag

En trykkavlastningssystem for CO<sub>2</sub> er utformet for å ventilere CO<sub>2</sub> fra et system hvor trykket er høyere enn et gitt maksimumstrykk. Forholdsregler må tas når du utformer et trykkavlastningssystem for CO<sub>2</sub> for å unngå dannelse av tørris og blokkering av sikkerhetsventilen og nedstrøms avlastningsrør.

En simuleringsmodell for nedstrøms avlastningsrør ble utviklet for å evaluere utviklingen av trykket ved et nedstrøms avledningsrør av et trykkavlastningssystem. Med vekt på kjølesystemer for supermarkeder ble et nedstrøms avlastningsrør med geometri basert på et system som brukes i industrien implementert i modellen. Simuleringsmodellen er basert på Martinelli-Nelson to-fase ligning for trykktap. Beregningsmetoden ble validert ved å sammenligne med tidligere eksperimentell forsøk med samme massefluks og geometri. Varmeoverføring fra omgivelsene ble også tatt hensyn til i modellen.

Resultatene fra simuleringen ble sammenlignet med standarden NS-EN 13136, "Kuldeanlegg og varmepumper - Trykkavlastningsordninger og tilhørende rørledninger - Beregningsmetoder".

Simuleringsresultatene viser at den lave temperatur ved atmosfærisk trykk og dannelse av tørris når trykket nådde trippelpunktet var som forventet ut i fra teoretiske beregninger. For massefluks på 100-200 kg/sm<sup>2</sup> ble trippelpunktet nådd i den siste delen av nedstrømsrøret. For massefluks lavere enn 45 kg/sm<sup>2</sup> ble the trippelpunktet nådd i sikkerhetsventilen.

Det var en signifikant økning i hastighet mot slutten av nedstrømsrøret på grunn av en reduksjon i tettheten. Med en varmebelastning på over 36 kW (G=200 kg/sm<sup>2</sup>) og nedstrøms rørdiameter på 40 mm ble utløpshastigheten sonisk (Ma>0.3).

Trykktapet i et nedstrøms rør øker med økende massefluks. Utløpsstrømningshastigheten øker også med økende massefluks. For å unngå tørris dannelse i sikkerhetsventilen, og for å ha en effektiv trykkavlastningsprosess bør massefluksen være så høy som mulig, men uten å gi sonisk strømningshastighet ved utløpet.





# Preface

This master thesis is the final work of a five year Master Degree Program at the Department of Energy and Process Engineering at NTNU.

The thesis investigates different pressure release systems for CO<sub>2</sub> with emphasis on possible hazards for pressure release concepts proposed in the industry.

I would like to thank my supervisor Petter Nekså for his helpful guidance through this work. Further, I would like to thank my co-supervisors Håvard Rekstad and Geir A. Owren for great discussions and valuable input. I would also like to thank Hans T. Haukås for giving me inspiration through his dedication on this topic.



# Contents

<b>Abstract</b>	<b>i</b>
<b>Sammendrag</b>	<b>ii</b>
<b>Preface</b>	<b>iv</b>
<b>Nomenclature</b>	<b>ix</b>
<b>List of Figures</b>	<b>xii</b>
<b>List of Tables</b>	<b>xiv</b>
<b>1 Introduction</b>	<b>1</b>
1.1 Thermodynamic properties of CO <sub>2</sub> . . . . .	1
1.2 Formation of solid CO <sub>2</sub> . . . . .	3
1.3 Main goal . . . . .	4
<b>2 Pressure release of CO<sub>2</sub></b>	<b>5</b>
2.1 General theory on pressure release . . . . .	5
2.1.1 Isentropic process . . . . .	5
2.1.2 Isenthalpic process . . . . .	6
2.1.3 Compressible flow . . . . .	6
2.1.4 Two-phase flow . . . . .	6
2.2 Theoretical calculations . . . . .	7
2.3 Dry ice formation, deposition and blockage . . . . .	8
2.3.1 Experiment on the blockage possibilities and danger of CO <sub>2</sub> releasing . . . . .	9
2.3.2 Pressure relief system in supermarket refrigeration - Advansor	10
2.3.3 Periodic blockage . . . . .	11

2.3.4	Experimental observation of sedimentation phenomena of CO <sub>2</sub> dry ice in model channel . . . . .	11
2.4	Possible hazards . . . . .	11
<b>3</b>	<b>Design of safety relief systems</b>	<b>13</b>
3.1	Existing design - Diplom-Is . . . . .	13
3.2	Possible measures to avoid formation of dry ice and blockage of downstream pipes . . . . .	14
<b>4</b>	<b>Analysis of pressure development through a pressure relief system</b>	<b>17</b>
4.1	Two-phase flow pressure drop . . . . .	17
4.1.1	The frictional pressure drop . . . . .	18
4.1.2	Pressure drop in bends . . . . .	20
4.2	Thermodynamic data . . . . .	20
4.3	Analysis of heat transfer from ambient air to downstream pipe dur- ing pressure release of CO <sub>2</sub> . . . . .	20
4.4	Calculation of pressure drop according to relevant standard . . . . .	21
4.4.1	Calculations according to NS-EN 13136 . . . . .	22
4.4.2	Pressure loss coefficient . . . . .	22
4.4.3	Critical area . . . . .	22
4.5	Reliability of calculation model . . . . .	22
<b>5</b>	<b>Results</b>	<b>25</b>
5.1	Pressure drop . . . . .	25
5.2	Heat transfer . . . . .	30
5.3	Pressure drop - EN 13136 . . . . .	30
<b>6</b>	<b>Discussion</b>	<b>33</b>
<b>7</b>	<b>Experimental setup</b>	<b>37</b>
7.1	Experiments . . . . .	37
<b>8</b>	<b>Conclusion</b>	<b>39</b>
	<b>Bibliography</b>	<b>40</b>
	<b>Appendices</b>	<b>43</b>
<b>A</b>	<b>Thermodynamic data</b>	<b>45</b>
A.1	Thermophysical properties of CO <sub>2</sub> . . . . .	45
A.2	Thermophysical properties of air . . . . .	45
<b>B</b>	<b>Ts-diagram</b>	<b>47</b>





# Nomenclature

## Abbreviations

*GWP* Global Warming Potential

*ODP* Ozone Depleting Potential

*CRB* Centerline Radius of Bend

## Greek letters

$\alpha$	Thermal diffusivity	$\text{m}^2/\text{s}$
$\beta$	Volumetric thermal expansion coefficient	$1/\text{K}$
$\mu$	Dynamic viscosity	$\text{kg}/\text{sm}$
$\nu$	Kinematic viscosity	$\text{m}^2/\text{s}$
$\zeta$	Pressure loss coefficient	-
$\kappa$	Isentropic exponent	-
$\varphi$	Density of heat flow rate	$\text{kW}/\text{m}^2$
$\rho$	Density	$\text{kg}/\text{m}^3$
$\rho_H$	Homogeneous density	$\text{kg}/\text{m}^3$
$\theta$	Bend angle	$^\circ$

## Roman letters

A	Area	$\text{m}^2$
a	Speed of sound	$\text{m}/\text{s}$
C	Function of the isentropic exponent	-

D	Pipe diameter	m
$f_D$	Darcys friction factor	-
$f_{LO}$	Fanning friction factor	-
G	Mass flux	kg/sm <sup>2</sup>
$\bar{h}$	Average heat convection coefficient	W/m <sup>2</sup> K
$\Delta h_{vap}$	Specific heat of vaporization	kJ/kg
h	Specific enthalpy	kJ/kg
k	Thermal conductivity	W/mK
$K_b$	Theoretical capacity correction factor for sub-critical flow	-
$k_b$	Bend loss coefficients	-
$K_{dr}$	De-rated coefficient of discharge	-
L	Pipe length	m
Ma	Mach-number	-
$\overline{Nu}_D$	Nusselt number	-
$\Delta p_a$	Acceleration pressure drop	bar
$\Delta p_f$	Frictional pressure drop	bar
$\Delta p_g$	Gravitational pressure drop	bar
$P_0$	Inlet pressure	bar
$P_c$	Critical pressure	bar
Pr	Prandtl number	-
$q_{conv}$	Total heat loss by convection	W
$Q_{md}$	Minimum required discharge capacity of the pressure relief device	kg/h
$\rho$	Density	kg/m <sup>3</sup>
$Ra_D$	Rayleigh number	-
$R_b$	Bend radius	m



Re	Reynolds number	-
$T_{\infty}$	Ambient temperature	$^{\circ}\text{C}$
$T_{sur}$	Surrounding temperature	$^{\circ}\text{C}$
$T_s$	Surface temperature	$^{\circ}\text{C}$
u	Velocity	m/s
s	Specific entropy	kJ/kgK
v	Specific volume	$\text{m}^3/\text{kg}$
x	Vapor quality	-

### Subscripts

0	Inlet
0,in	Inlet stagnation state
c	Critical
g	Gas
l	Liquid
LO	Liquid only
s	Solid
SP	Single-phase
TP	Two-phase
tt	turbulent-turbulent



# List of Figures

1.1	Phase diagram of $CO_2$ . . . . .	2
1.2	Pressure-Enthalpy diagram of $CO_2$ . . . . .	3
2.1	Pressure release of saturated liquid and saturated gas at 60 bars. . .	7
2.2	Downstream pipe system of a pressure relief system. . . . .	10
3.1	Upstream heating. . . . .	14
3.2	Multistage heating. . . . .	15
3.3	Downstream heating. . . . .	16
5.1	A pressure relief system with downstream pipe. . . . .	26
5.2	Pressure drop per pipe length. . . . .	27
5.3	Homogeneous density, $\rho_H$ , per pipe length . . . . .	28
5.4	Homogeneous velocity, $u_H$ , per pipe length . . . . .	29
B.1	Temperature-Entropy diagram of $CO_2$ . . . . .	47
C.1	Screenshot from video by Advansor. . . . .	49
C.2	Screenshot from video by Advansor. . . . .	50



# List of Tables

1.1	Properties of refrigerants . . . . .	2
2.1	Expansion of CO <sub>2</sub> . . . . .	8
2.2	Nuova high pressure safety valve . . . . .	10
3.1	Heating . . . . .	15
4.1	Calculated downstream pressure . . . . .	23
4.2	Downstream pressure from experiments . . . . .	23
4.3	Comparison of data . . . . .	23
4.4	Mass flux . . . . .	24
5.1	Input data . . . . .	25
5.2	Pressure loss in downstream pipe . . . . .	26
5.3	Heat transfer in downstream pipe . . . . .	30
5.4	Pressure loss in downstream pipe - EN 13136 . . . . .	30
5.5	Outlet velocity . . . . .	31
A.1	Thermodynamic properties of CO <sub>2</sub> . . . . .	45
A.2	Thermodynamic properties of air at atmospheric pressure . . . . .	46



# Chapter 1

## Introduction

Carbon dioxide ( $\text{CO}_2$ ) is a natural substance and is at gas state at standard temperature and pressure. It exists in the atmosphere at a concentration of 0.04 % by volume.

$\text{CO}_2$  is widely used in the industry and systems with large amounts of  $\text{CO}_2$  are found for example in the refrigeration industry and in the petroleum industry.

Together with ammonia ( $\text{NH}_3$ ),  $\text{CO}_2$  was the dominating refrigerant in the refrigeration industry until synthetic refrigerants was introduced in 1938 [9]. After being abandoned for almost 40 years,  $\text{CO}_2$  was reintroduced as a refrigerant in the mid 90s [12] due to the synthetic refrigerants' ozone depletion and greenhouse effect which was highly focused in the Montreal Protocol [17].  $\text{CO}_2$  also had the advantage of being non-toxic and non-flammable, unlike ammonia (toxic) and hydrocarbons (flammable). The development the last decades has shown that  $\text{CO}_2$  is competitive both technically and economically to other refrigerants.

In the petroleum industry, pipe transport of large amounts of  $\text{CO}_2$  is common. Pressurized liquid  $\text{CO}_2$  is transported from the process plant through pipes to the reservoir for enhanced oil recovery (EOR) or for storage.

### 1.1 Thermodynamic properties of $\text{CO}_2$

$\text{CO}_2$  is a non-flammable and non-toxic natural refrigerant with no Ozone Depletion Potential(ODP) and negligible Global Warming Potential(GWP). The refrigerant properties of  $\text{CO}_2$  are quite different from other conventional refrigerants, as shown in Table 1.1.

One important difference is the volumetric capacity which is much larger than for synthetic refrigerants. The large volumetric capacity allows smaller components for

Table 1.1: Properties of refrigerants

Refrigerant	R744	R717	R134a
Molecular	CO <sub>2</sub>	NH <sub>3</sub>	CH <sub>2</sub> FCF <sub>3</sub>
ODP	0	0	0
GWP	1	0	3100
Critical temperature $t_c$ [°C]	31.1	133.0	101.7
Critical pressure $p_c$ [MPa]	7.38	11.42	4.055
Boiling point temperature, $t_s$ [°C]	-78.4	-33.3	-26.2
Volumetric refrigeration capacity at 0°C[kJ/m <sup>3</sup> ]	22600	4360	2860

refrigeration systems even though the vapor pressure is much higher. The critical point and triple point can be seen in the phase diagram in Figure 1.1.

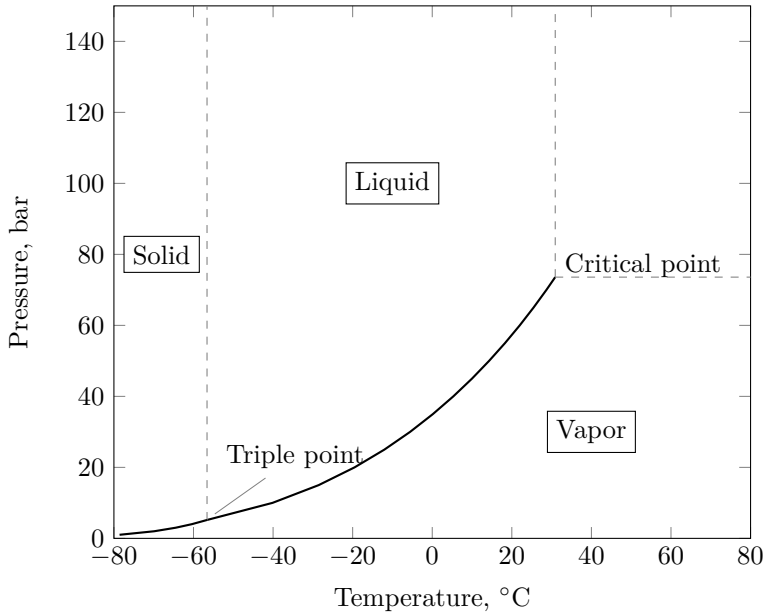


Figure 1.1: Phase diagram of  $CO_2$

Critical pressure and temperature of  $CO_2$  is 7.38 MPa (73.8 bar) and 31.1°C, respectively. Above the critical temperature it is not possible to transfer heat to the ambient by condensation, which is normal in conventional refrigeration processes. If the ambient temperature is higher than the critical temperature the heat transfer occurs in a gascooler at the high pressure side of a refrigeration system. This is called a transcritical refrigeration cycle and heat is transferred at gliding temperature above the critical point.



The pressure and temperature at the triple point is 0.518 MPa (5.18 bar) and  $-56.6^{\circ}\text{C}$ , respectively. The saturation pressure at  $0^{\circ}\text{C}$  is 3.5 MPa and it gives a reduced pressure of 0.47 at  $0^{\circ}\text{C}$ . This is much higher than for the conventional refrigerants and means that  $\text{CO}_2$  refrigeration cycles will operate closer to the critical point.

## 1.2 Formation of solid $\text{CO}_2$

Formation of dry ice (solid  $\text{CO}_2$ ) during pressure release is a known phenomena, and it can be illustrated in a phase-diagram like Ts-diagram or Ph-diagram, see Figure 1.2. Dry ice might be formed when the pressure reaches the triple point of 5.18 bar.

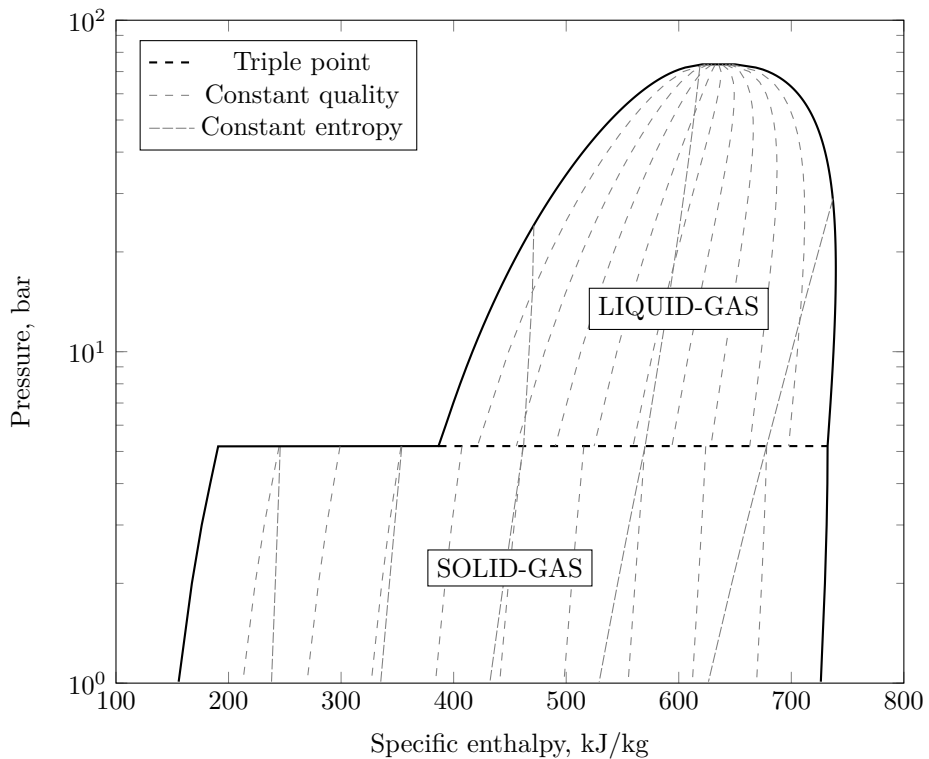


Figure 1.2: Pressure-Enthalpy diagram of  $\text{CO}_2$

### 1.3 Main goal

The main goal for this report is to develop a simulation model for flow of CO<sub>2</sub> through a downstream pipe system of a pressure release valve in order to better understand the possible hazards related to pressure release of CO<sub>2</sub>. The results will be discussed from a safety point of view in relation to the standard NS-EN 13136.

# Chapter 2

## Pressure release of CO<sub>2</sub>

Pressurized CO<sub>2</sub> can be found in many systems and for safety reasons these systems have to handle a possible situation where the system have to be vented. It can be in case of an emergency like open fire or damages on the system equipment or for maintenance. Venting pressurized CO<sub>2</sub> to atmospheric pressure, which is lower than the triple point, might lead to formation of dry ice.

### 2.1 General theory on pressure release

#### 2.1.1 Isentropic process

An isentropic process is an ideal process where the entropy remains constant. An isentropic process is reversible and adiabatic.

#### Reversible process

*“A process of a system is reversible if the system and all parts of its surroundings can be exactly restored to their respective initial states after the process has taken place”*

Fundamentals of Engineering Thermodynamics, [14]

No process that involves an unrestrained expansion of a gas or liquid can be reversible, but a process that is perfectly executed is approximately reversible. An example is gas through a properly designed nozzle or diffuser.

### 2.1.2 Isenthalpic process

An isenthalpic process is an irreversible process without any change in enthalpy. As the fluid expands during the process there will usually be a significant change in pressure and temperature. An isenthalpic process is by definition adiabatic, has no exchange of work with the surroundings and has no change in kinetic energy of the fluid.

### 2.1.3 Compressible flow

A gas that has a velocity that is comparable to its speed of sound will have a significant change in density and the flow is termed compressible. The Mach-number is defined as follows:

$$Ma = \frac{V}{a} \quad (2.1)$$

where  $V$  is the velocity of the gas and  $a$  is the speed of sound of the gas. The textbook Fluid Mechanics [21] defines a flow with Mach-number lower than 0.3 as an incompressible flow. A flow with Mach-number higher than 0.3 is a sonic flow and density changes is more and more important as the Mach-number increases.

Choking in a system is defined as the maximum mass flow rate as a function of downstream pressure. The flow will have its maximum speed at the smallest cross-section area.

The critical pressure ratio is given by Equation 2.2:

$$\frac{P_c}{P_0} = \left( \frac{2}{\kappa + 1} \right)^{\frac{\kappa}{\kappa - 1}} \quad (2.2)$$

where  $\kappa$  is the adiabatic exponent.

### 2.1.4 Two-phase flow

Liquid-gas two-phase mixture of  $\text{CO}_2$  exists between the saturation lines from the triple point up to the critical point. Below the triple point it is solid-gas two-phase mixture. When depressurizing  $\text{CO}_2$  both liquid-gas two-phase flow and solid-gas two-phase flow might exist before reaching atmospheric pressure.

## 2.2 Theoretical calculations

In this part theoretical calculations for pressure release of  $\text{CO}_2$  will be presented. Figure 2.1 illustrates the pressure release process of  $\text{CO}_2$  from saturated liquid and saturated gas at 60 bar. The red lines are isentropic expansion and the blue lines are isenthalpic expansion. The expansion through the safety valve is an isentropic process as the flow accelerates through the smallest cross-section area, but as the flow reaches the downstream pipe the kinetic energy dissipates to internal energy and the flow becomes isenthalpic. For the rest of this report pressure release through safety relief valve and downstream pipe is considered isenthalpic.

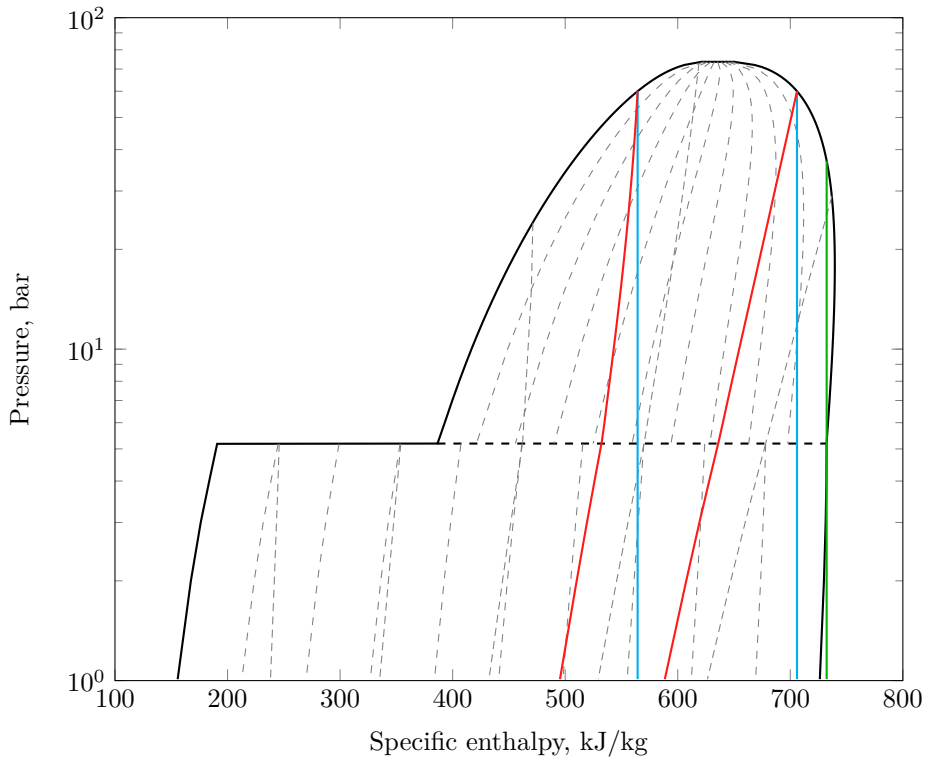


Figure 2.1: Pressure release of saturated liquid and saturated gas at 60 bars.

As Figure 2.1 illustrates, the amount of dry ice formed during expansion from the two-phase region depends on upstream pressure and vapor quality. Dry ice formation during expansion from sub cooled liquid or superheated gas is dependent on pressure and temperature. Above the critical pressure there is no phase change and formation of dry ice during expansion of critical  $\text{CO}_2$  is only depending on temperature. Table 2.1 shows pressure release from different pressures and upstream vapor qualities.

Table 2.1: Expansion of CO<sub>2</sub>

$P_0$ bar	$x_0$ [-]	$x_{triple}$ [-]	$x_{atm}$ [-]	$v_{solid},\%$ [%]	$m_{solid},\%$ [%]
60	1	0.95	0.96	0.007	4
50	1	0.98	0.99	0.002	1
40	1	-	-	0.00	0
30	1	-	-	0.00	0
20	1	-	-	0.00	0
10	1	-	-	0.00	0
60	0	0.69	0.71	0.072	29
50	0	0.64	0.67	0.089	33
40	0	0.60	0.63	0.107	37
30	0	0.55	0.58	0.130	42
20	0	0.49	0.53	0.161	47
10	0	0.42	0.46	0.215	54

Independent on the type of expansion process, solid CO<sub>2</sub> may form when the pressure reaches the triple point. The amount varies from 0 %(mass) to over 50 %. On the other hand, the volumetric fraction of dry ice formed are quite small, and range from 0 % to 0.22 %. Despite the low volumetric fraction, dry ice may deposit and, as the expansion process goes on upstream the deposition, blockage may occur.

However, since the saturated gas line in the Ph-diagram has a slightly bend over the triple point there is as maximum pressure for which no dry ice is formed during pressure release of saturated gas to atmospheric pressure, assuming isenthalpic process. This pressure is approximately 37 bar as illustrated by the green line in Figure 2.1. During release of saturated gas at 37 bar the vapor quality at the triple point is 1 and there will be slightly superheated gas at atmospheric pressure, according to the Ph-diagram.

## 2.3 Dry ice formation, deposition and blockage

Dry ice can be formed in the relief valve or in the downstream pipes. The geometry of the relief valve and the downstream pipe system decides whether and how much dry ice that deposits.

### **2.3.1 Experiment on the blockage possibilities and danger of CO<sub>2</sub> releasing**

In [6], different experiments on blockage possibilities has been done. Experiments with CO<sub>2</sub> releasing under worst flow conditions (saturated liquid) were done and three different test sections were used to configure worst working conditions with meander tubes with small diameter (12mm, unfortunately no mass-flow is given for these experiments, only regulating valve opening). Further follows description of the experimental results.

#### **Design of experimental setup**

The test rig consists of two CO<sub>2</sub> cylinders, a regulating valve and instruments for measuring pressure and temperature. CO<sub>2</sub> vapor and liquid are drawn from a CO<sub>2</sub> vapor cylinder and a CO<sub>2</sub> liquid cylinder. A valve on each cylinder regulates the mass flow. Vapor and liquid CO<sub>2</sub> are mixed and flows into a regulating valve. A copper tube is installed before the test section downstream of the regulating valve. The temperature and pressure are measured upstream and downstream of the regulating valve.

#### **Sudden expansion downstream pipe**

When releasing saturated liquid at 64 bar pressure, formation and deposition of solid CO<sub>2</sub> were observed downstream the releasing valve when the pipe had sudden expansion from 4 mm to 25 mm. The solid CO<sub>2</sub> even blocked the pipe fully under certain conditions. As a consequence of full blockage of the small plastic tube used in the experiment, the plastic tube got broken. Where the solid CO<sub>2</sub> locates is decided by the mass-flow rate. For small mass-flow rates, the solid CO<sub>2</sub> locates far away from the sudden expansion, and when increasing the mass-flow rate the solid CO<sub>2</sub> deposited both at the sudden expansion and further down. When increasing the mass-flow rate even more, the solid CO<sub>2</sub> only locates at the sudden expansion.

#### **Meander tubes, 90° and 60°**

Releasing of saturated liquid at 61 bar pressure through meander tube downstream of releasing valve leads to formation and possibilities for deposition of solid CO<sub>2</sub>. Increasing the opening of the regulating valve, less CO<sub>2</sub> is deposited in the meander tubes. Experiments showed that it is an optimal velocity of CO<sub>2</sub> for which all the formed solid CO<sub>2</sub> will be carried away by the CO<sub>2</sub> vapor.

Table 2.2: Nuova high pressure safety valve

Model	$d_0$ [mm]	Discharge coefficient [-]
E10	10	0.85
E14	14	0.89

### 2.3.2 Pressure relief system in supermarket refrigeration - Advansor

Advansor is a Danish company that provides thermal systems for production of heating and cooling using  $\text{CO}_2$  as refrigerant. As a part of the system the releasing safety valve needs to be tested to see if it works properly. Advansor have done tests where the aim is to see if there is any tendency to blocking or buildup of solid  $\text{CO}_2$  in the downstream pipes after the safety valve.

In the test they use a 60 bar pressure relief valve from Nuova (see Table 2.2 for more specifications on the valve[16]), with a capacity of 4776 kg/h, and it is placed at the top of a 130 L receiver tank (2 m<sup>2</sup> surface area) with 20 kW heat load from circulation hot water in an internal coil. This corresponds to an ambient open fire with 10 kW/m<sup>2</sup> effect. A 1.8 meter long hose (36 mm diameter) connects the safety valve to the downstream pipe system. The downstream pipe is 11 meter long in total (40 mm diameter) and consists of 10 elbow bends. See Figure 2.2.



Figure 2.2: Downstream pipe system of a pressure relief system.

During the test the safety valve releases 10 kg  $\text{CO}_2$  within 30 seconds, which corresponds to 47 kW ( $\Delta h_{vap}=140.5$  kJ/kg). As expected, some dry ice was formed during the pressure release. Since the flow velocity of the released  $\text{CO}_2$  was very



high the dry ice did not accumulate in the downstream pipe. The hose after the safety valve became very cold, but it did not get any damages.

Unlike the experiments in [6] which released saturated liquid  $\text{CO}_2$  with tricky downstream geometry conditions, Advansor released saturated gas through more favorable downstream pipe system.

### 2.3.3 Periodic blockage

Experiments done by Dongping [6] on pressure release of  $\text{CO}_2$  through a needle valve shows that under certain upstream conditions the downstream pressure will follow a periodic pattern. Four stages were observed in the pattern:

1. Pressure when there is no blockage in the downstream pipe.
2. Process of the downstream pressure increasing as blockage occurs.
3. Pressure when there is blockage in the downstream pipe.
4. Process of the downstream pressure decreasing as dry ice melts and disappears.

As dry ice deposits the pressure upstream the deposition will increase. When the pressure reaches the triple point of 5.18 bar dry ice will not longer form, but there will be a mixture of gas and liquid with higher temperature than the dry ice and the deposited dry ice will start to melt/sublimate. It is also observed that large blocks of solid  $\text{CO}_2$  blow away suddenly as it is released from the pipe wall during the melting process.

### 2.3.4 Experimental observation of sedimentation phenomena of $\text{CO}_2$ dry ice in model channel

In [22] the dynamic behavior of dry ice particles with different shapes of the downstream expansion channel is investigated. Experiments show that the sedimentation phenomena decreases when the shape of the downstream expansion channel is changed from sudden expansion to a tapered channel. The experiments are done with respect to development of a refrigeration system with temperatures below the triple point of  $\text{CO}_2$ . The article concludes that when the shape of the evaporator is changed to a tapered channel the ultra-low temperature cascade refrigeration system works continuously and stably without dry ice blockage.

## 2.4 Possible hazards

The most significant possible hazard from formation of dry ice during depressurization of  $\text{CO}_2$  is blockage of relief valve and downstream pipes, which partially or

fully reduce the functionality of the pressure relief system. In case of total blockage of a safety relief system downstream pipes can get broken as Dongping [6] showed through her experiments.

Another possible hazard is the low temperatures that occurs as the pressure gets closer to the atmospheric pressure. Advansor [1] verified from their experiments that the downstream pipes gets very cold after pressure release, but the material could handle such low temperatures, at least for a short period.

Dongping [6] also discovered generation of static electricity from friction between  $\text{CO}_2$  gas and small particles of solid  $\text{CO}_2$ . The static electricity is reduced as the upstream vapor quality gets lower because more solid  $\text{CO}_2$  is formed and the solid  $\text{CO}_2$  particles become larger which leads to less friction between  $\text{CO}_2$  gas and solid  $\text{CO}_2$ .

The blockage process can be separated into two stages. First the formation of solid  $\text{CO}_2$  and then the deposition of the formed solid  $\text{CO}_2$ . The thermodynamic process determines the amount of solid  $\text{CO}_2$  formed and the flow characteristics determines whether solid  $\text{CO}_2$  deposits or not.

## Chapter 3

# Design of safety relief systems

### 3.1 Existing design - Diplom-Is

Diplom-Is is a company that produces ice cream and has a big storage hall at Hegstadmyra south of Trondheim. They have a CO<sub>2</sub> refrigeration system operating at pressures up to 120 bar and performs a cooling effect of 300 kW, depending on ambient temperature.

Safety relief valves are placed at suction side of low-pressure and high-pressure compressors, discharge side of high-pressure compressors and two at the receiver tank. They have design pressure at 30 bar, 45 bar, 120 bar, 60 bar and 90 bar, respectively.

Under normal conditions the receiver tank is connected to a 60 bar safety relief valve, while at abnormal conditions like accumulation of refrigerant in the tank a 90 bar safety relief valve is connected. Pressure release of saturated gas at 60 bar will lead to formation of dry ice when the triple point is reached. At 90 bar the pressure is higher than the critical point and the amount of dry ice formed during pressure release is decided by the temperature. Both safety relief valves at the receiver releases CO<sub>2</sub> directly out to the room, without any downstream pipe, because eventual formed dry ice can deposit and block the pipe. Both safety relief valves at the suction side of the compressors will release superheated vapor when the system is operating and no dry ice will be formed. Even at standstill superheated vapor will be released because the saturation temperature is lower than the temperature inside the room.

Downstream pipes lead the released CO<sub>2</sub> from the 45 bar and 30 bar safety release valves to a manifold, before it is lead out of the room. Formation of dry ice from

releasing saturated gas at 45 and 30 bar is not considered a threat to blockage of downstream pipes.

### 3.2 Possible measures to avoid formation of dry ice and blockage of downstream pipes

Looking at the expansion processes in Figure 2.1 dry ice is likely to form when releasing depressurized CO<sub>2</sub>. The specific enthalpy at atmospheric pressure is lower than the specific enthalpy for saturated gas at the triple point. In some way, heat have to be added to the CO<sub>2</sub> in order to have saturated gas at atmospheric pressure.

To avoid formation of dry ice heat have to be added to the flow before the pressure reaches the triple point. Another possible solution is to add head to melt the formed dry ice. Figure 3.1 and Figure 3.2 shows in a Ph-diagram different possibilities to avoid dry ice formation by adding heat before the pressure reaches the triple point.

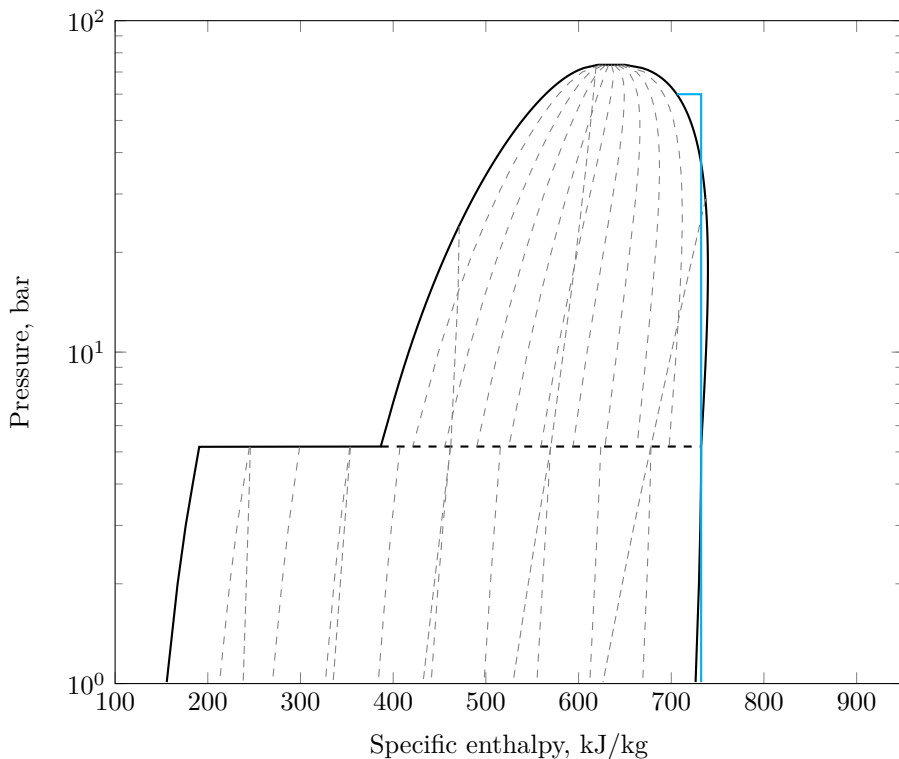


Figure 3.1: Upstream heating.

Another solution is to add heat at atmospheric pressure as illustrated in Figure 3.3

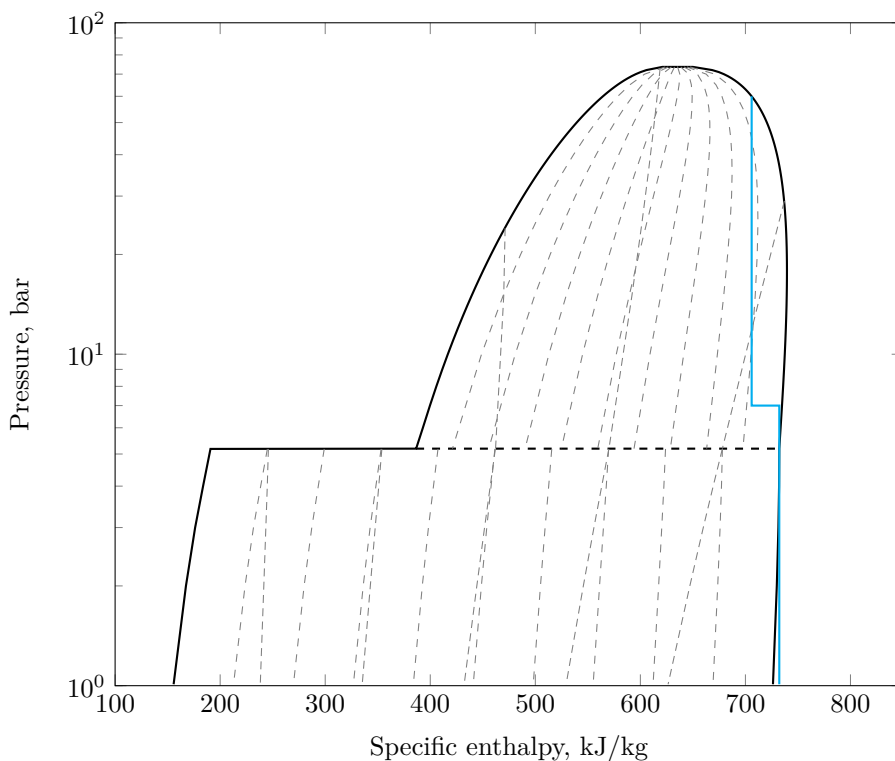


Figure 3.2: Multistage heating.

The amount of heat that needs to be added is shown in Table 3.1. Pressure release of saturated gas at 60 bar and mass flow according to a heat load of 20 kW (0.1412 kg/s).

Table 3.1: Heating

Solution	$\Delta h$ [kJ/kg]	$\Delta H$ [kW]
Upstream heating	26.30	3.71
Multistage heating	26.30	3.71
Downstream heating	20.30	2.87

As can be seen from Figure 3.1, Figure 3.2 and Table 3.1 there is a need of almost 4 kW heat to avoid dry ice formation which is relatively high and impossible to achieve by free convection at normal room temperature, see Chapter 5. The heat needed to melt the formed dry ice in the case of downstream heating is less than for the two other cases because saturated gas at atmospheric pressure has lower specific enthalpy than saturated gas at the triple point.

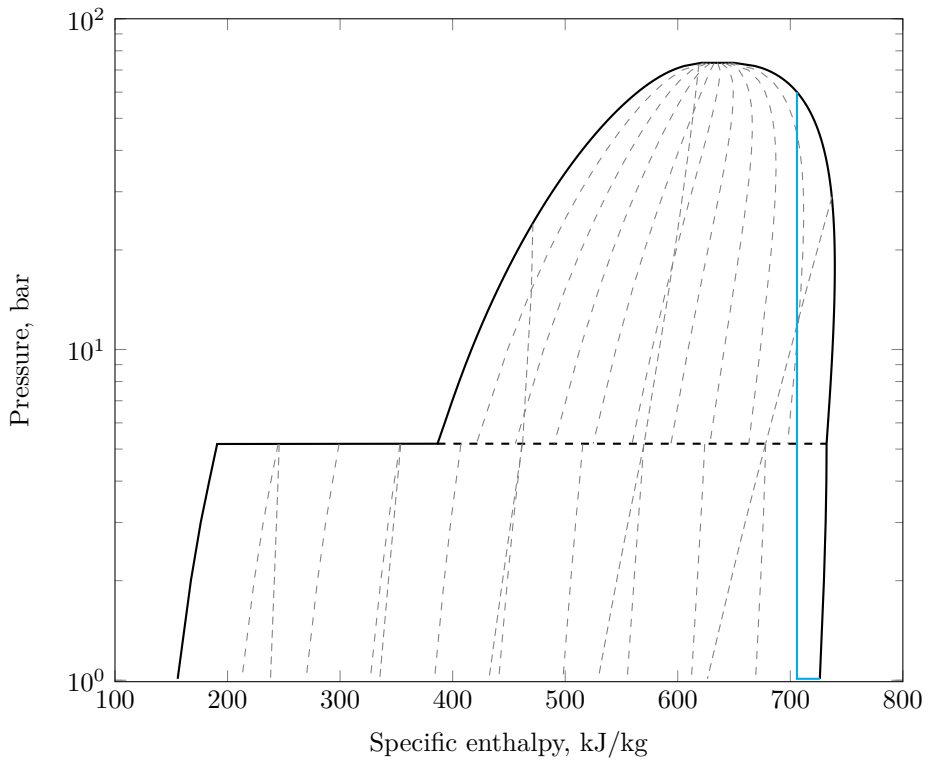


Figure 3.3: Downstream heating.

In the case of downstream heating, Figure 3.3, dry ice will be formed and the external heat is needed to sublimate the dry ice. This is the solutions that requires least external heating, but there is a possibility that the dry ice will accumulate faster than the external heat is able to sublimate the dry ice which can lead to blockage of the pipe.

Another question is how to implement this kind of external heat to the pressure relief system. Dongping [6] suggested to add a heat membrane inside the safety valve on the seat and disc. This is not enough to sublimate all of the dry ice, but it may prevent blockage.

## Chapter 4

# Analysis of pressure development through a pressure relief system

In this chapter the pressure development downstream the safety valve in a CO<sub>2</sub> refrigeration system will be investigated. The pressure relief system from Advansor will be used as a basis for the geometry. This system is tested and filmed by Advansor and a similar one is also installed at Diplom-Is at Hegstadmyra in Trondheim.

The aim of this analysis is to investigate the impact of geometry and flow characteristics on dry ice formation in a safety relief system and compare the results with a relevant standard (NS-EN 13136) [8].

### 4.1 Two-phase flow pressure drop

In calculation of pressure drop in a two-phase flow there are two main calculation models. It is the homogeneous model and the separated flow model.

The homogeneous model considers the gas and liquid are in equilibrium and that their respective velocities are equal (slip ratio=1). The frictional pressure drop is calculated as if it was single phase flow and the properties inside the single phase friction coefficient are modified. The homogeneous model works best for high velocities.

The separated flow model considers the two phases to flow separately and have different velocity.

Calculations show that the flow velocity through the downstream pipe is high and increasing as the pressure drops because the density of carbon dioxide gas is decreasing. The high speed is also confirmed looking at video from pressure release test done by Advansor. Thus, using the homogeneous flow model should be a good assumption.

The homogeneous density is given as:

$$\rho_H = \frac{\rho_g \rho_l}{x \rho_l + (1 - x) \rho_g} \quad (4.1)$$

The pressure drop of fluid flow through a pipe is the sum of the frictional pressure drop, the acceleration pressure drop and the gravitational pressure drop.

$$\Delta p = \Delta p_f + \Delta p_a + \Delta p_g \quad (4.2)$$

In this report only the frictional pressure drop will be considered as it is the dominating contribution to the total pressure loss.

### 4.1.1 The frictional pressure drop

#### Single-phase

The frictional pressure drop for a single-phase flow is given by the equation:

$$\Delta p_f = f_D \frac{L}{D} \frac{\rho u^2}{2} \quad (4.3)$$

where  $f_D$  is the Darcy Friction Factor which for turbulent flow and using Blasius correlation is:

$$f = 0.316 Re^{-\frac{1}{4}} \quad (4.4)$$

#### Two-phase

The frictional pressure drop for a two-phase flow is calculated as if the flow is a single-phase flow, but with modifications on the properties inside the single-phase friction coefficient. Lockhart-Martinelli (1947), [11], defined the two-phase multipliers:

$\phi_L^2$  = ratio of the two-phase frictional pressure gradient to the frictional pressure gradient if liquid flows alone

$\phi_{LO}^2$  = ratio of the two-phase frictional pressure gradient to the frictional pressure gradient if total mixture flows as a liquid



They expressed the frictional pressure gradient per unit length as follows:

$$\left(\frac{\Delta P}{\Delta L}\right)_{TP} = \phi_{LO}^2 \left(\frac{\Delta P}{\Delta L}\right)_l \quad (4.5)$$

where

$$\left(\frac{\Delta P}{\Delta L}\right)_l \quad (4.6)$$

is the pressure gradient per unit length if the liquid phase is assumed to flow alone.

The overall frictional pressure drop on integral form is then:

$$\Delta p_f = \Delta p_{LO} \left( \frac{1}{\Delta x} \int \phi_{LO}^2 dx \right) \quad (4.7)$$

Martinelli-Nelson (1948), [13], expressed the two-phase multiplier as follows:

$$\phi_{LO}^2 = 12.82 X_{tt}^{-1.47} (1-x)^{1.8} \quad (4.8)$$

Assuming smooth pipe and that both phases are turbulent flow they defined  $X_{tt}$  as:

$$X_{tt} = \left(\frac{1-x}{x}\right)^{0.9} \left(\frac{\rho_g}{\rho_l}\right)^{0.5} \left(\frac{\mu_l}{\mu_g}\right)^{0.1} \quad (4.9)$$

The frictional pressure drop is given by:

$$\Delta p_{LO} = \frac{2f_{LO}G^2L}{\rho_l D} \quad (4.10)$$

where  $f_{LO}$  is the liquid friction factor (Fanning) for smooth tubes:

$$f_{LO} = \frac{0.079}{Re_{LO}^{0.25}} \quad (4.11)$$

The frictional pressure drop is then:

$$\Delta p_f = 12.82 X_{tt}^{-1.47} (1-x)^{1.8} \frac{2f_{LO}G^2L}{\rho_l D} \quad (4.12)$$

### 4.1.2 Pressure drop in bends

The pressure losses in a fluid flowing through a bend are due to both friction and momentum because of change in the direction of the flow. These two factors depends on the bend angle, the curvature ratio and the Reynolds number, and can be expressed as the sum of two components. The first component is the pressure drop resulting from friction in a straight pipe with equivalent length and depends on the Reynolds number. The second component is the losses due to changes of direction and depends on the curvature ratio and the bend angle.

The pressure loss of a single phase flow through a bend can be calculated as follows:

$$\Delta p = \frac{1}{2}f_D\rho u^2 \frac{\pi R_b}{D} \frac{\theta}{180^\circ} + \frac{1}{2}k_b\rho u^2 \quad (4.13)$$

No exact method exists for calculation pressure loss in two-phase flow through a bend. A normal solution is to multiply the single-phase pressure loss by a two-phase multiplier. The following method was proposed by Chisholm in 1980, [3], based on empirical correlations:

$$\frac{\Delta p_{TP}}{\Delta p_{LO}} = 1 + \left( \frac{\rho_L}{\rho_g} - 1 \right) \left[ \left\{ 1 + \frac{2.2}{k_{LO} \left( 2 + \frac{R_b}{D} \right)} \right\} (1 - x) + x^2 \right] \quad (4.14)$$

where  $\Delta p_{LO}$  is the pressure drop if the flow was a single-phase liquid flow.

## 4.2 Thermodynamic data

See Appendix A

### 4.3 Analysis of heat transfer from ambient air to downstream pipe during pressure release of CO<sub>2</sub>

As a part of the simulation of pressure development through the downstream pipe system, heat transfer from the ambient is also considered. Assuming free convection from the ambient air and assuming that the thin plastic pipe wall has the same temperature as the CO<sub>2</sub> flow.

The total heat loss can be calculated by Newton's law of cooling:

$$q_{conv} = \bar{h}\pi DL(T_\infty - T_{sur}) \quad (4.15)$$

The next equations are based on empirical correlations for external free convection flow and are found in [10].

Average heat convection coefficient for an isothermal cylinder [15]:

$$\bar{h} = \frac{k}{D} \overline{Nu}_D = C Ra_D^n \quad (4.16)$$

Where the Rayleigh number is:

$$Ra_D = \frac{g\beta(T_\infty - T_s)D^3}{\nu\alpha} \quad (4.17)$$

Average Nusselt number [4]:

$$\overline{Nu}_D = \left\{ 0.60 + \frac{0.387 Ra_D^{1/6}}{[1 + (0.699/Pr)^{9/16}]^{8/27}} \right\}^2 \quad Ra_D \leq 10^{12} \quad (4.18)$$

## 4.4 Calculation of pressure drop according to relevant standard

NS-EN 13136, Refrigerating systems and heat pumps - Pressure relief devices and their associated piping - Methods for calculation [8], is a standard suited to the specific requirements of refrigerating systems. According to this standard calculations are done on pressure drop in the downstream pipes. The same geometry and flow conditions as in Chapter 4 are used.

Some important notes from the standard:

- $h_{vap}$  is calculated at 1.1 times the set pressure of the pressure relief device
- The pressure loss in the downstream line shall not exceed:

$$\Delta p_{out} \leq 0.20 \times p_0 \quad (4.19)$$

where

$$p_0 = 1.1 p_{set} + p_{atm} \quad (4.20)$$

- The velocity in the upstream and downstream line shall not reach critical speed (sonic velocity)

In order to not exceed the maximum pressure loss in the downstream line the geometry of the downstream line is important. The downstream pipe have to be designed to handle the pressure release due to external heat load.

#### 4.4.1 Calculations according to NS-EN 13136

The pressure loss in the downstream pipe (from pressure relief valve to atmosphere) is given as:

$$\Delta p_{out} = p_1 - p_2 \quad (4.21)$$

where

$$p_1 = \sqrt{0.064\zeta \left[ \frac{A_c}{A_{out}} C K_{dr} K_b p_0 \right]^2 + p_2^2} \quad (4.22)$$

and

$$p_2 = p_{atm} \quad (4.23)$$

#### 4.4.2 Pressure loss coefficient

The pressure loss coefficient,  $\zeta$ , are calculated assuming smooth steel pipe and bend radius  $R=2D_R$ .

#### 4.4.3 Critical area

The critical area is given by:

$$A_c = \frac{Q_{md}}{0.2883 C K_{dr} K_b \sqrt{\frac{p_0}{v_0}}} \quad (4.24)$$

where the minimum required discharge capacity of the pressure relief device,  $Q_{md}$ , is given by:

$$Q_{md} = \frac{3600\varphi A_{surf}}{\Delta h_{vap}} \quad (4.25)$$

### 4.5 Reliability of calculation model

To verify that the calculation method described in this chapter is suitable for predicting pressure drop in a two-phase pipe flow, calculation results are compared with results from experiments done by Huang Dongping in [6]. All the calculations are based on the same geometry for the downstream test section with transparent plastic tube ( $D_d = 0.025m$  and  $L_d = 6m$ ).

See Table 4.1 for calculated data from this report and Table 4.2 for calculated and experimental data from [6]. For the experiment in Table 4.2 the mass flow rate is not given, but the ratio of the lift to the total lift ( $z/Z$ ) of the safety valve is given, and it is assumed that the mass-flow is in the same range. This assumption is based on the fact that an opening of 20 % of the valve corresponds to 0.007 kg/s and an opening of 90 % of the valve corresponds to 0.03 kg/s, which is described in [6].

Table 4.1: Calculated downstream pressure

Mass-flow [kg/s]	0.01	0.02	0.03
Downstream pressure [bar]	1.83	3.30	4.69

Table 4.2: Downstream pressure from experiments

$z/Z$	0.4	0.7
Downstream pressure [bar]	3	5.5

Another experiment from Dongping [7] is done and results from that compared to calculated values in this report is presented in Table 4.3. For this results the upstream pressure is  $p_{in}=57$  bar and the mass-flow rate is  $\dot{m}=0.021$  kg/s. The results are consistent and strengthens the reliability of the calculation model.

Table 4.3: Comparison of data

	Experiments	Calculations
Downstream pressure [bar]	4.20	4.08

In Table 4.4 the mass-fluxes are compared, and it can be seen that the mass-fluxes are in the same range.

In NS-EN 13136 the pressure loss in a bend, with bend radius of two times the pipe diameter, corresponds to the pressure loss in 0.6 m of pipe with diameter of 40 mm. Using Equation 4.13 and Equation 4.14 to calculate the pressure loss in bends with a heat load of 10 kW/m<sup>2</sup>, a bend corresponds to 0.38 m to 0.87 m of pipe depending on where the bend is placed.

Table 4.4: Mass flux

	Calculations	Experiments
Mass flux [kg/sm <sup>2</sup> ]	55-420	42-270

# Chapter 5

## Results

The results from the calculations described in Chapter 4 are presented in this chapter. The input parameters in Table 5.1 is applicable if nothing else is given.

Table 5.1: Input data

Symbol	Value
$P_{set}$ [bar]	60
$T_{amb}$ [K]	300
$A_{surf}$ [m <sup>2</sup> ]	2
$D_{d1}$ [mm]	36
$D_{d2}$ [mm]	40
$L_{d1}$ [m]	1.8
$L_{d2}$ [m]	11
Bend radius [mm]	5
Bend angle [°]	90
CRB/D	0.63
$k_b$	0.6
$\kappa$	1.3
C	2.63
$K_b$	1
$K_{dr}$	0.85 / 0.89

### 5.1 Pressure drop

The calculation model is based on the Martinelli-Nelson two-phase pressure drop equation on a two-phase flow in the downstream pipe system described in Figure 5.1. Equation 4.12 is used for both liquid-gas two-phase flow and solid-gas

two-phase flow, which means that the solid phase is treated as liquid phase with solid properties.

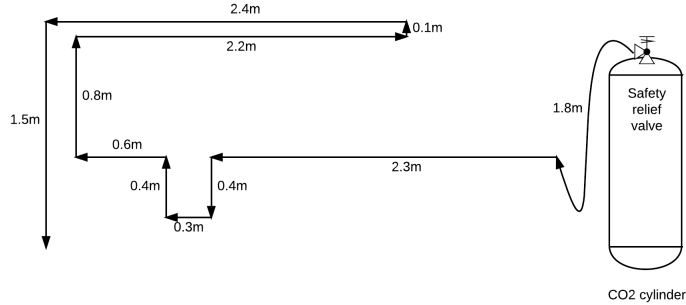


Figure 5.1: A pressure relief system with downstream pipe.

Figure 5.2 shows the pressure as a function of the length of the downstream pipe. The triple point is marked with a dashed line. The sudden drop in pressure that occurs ten times are due to bends and are calculated from Equation 4.13 and Equation 4.14. It can be observed that the pressure gradient is almost constant until it decreases rapidly at the end of the downstream pipe.

Figure 5.3 shows that the density is decreasing towards the end of the pipe and as a consequence the velocity increases significantly. In Figure 5.4 the velocity in the last part of the downstream pipe is presented. A dashed line shows the maximum allowed flow velocity according to the standard.

The pressure loss through the downstream pipe, the mass flow and the homogeneous velocity at the outlet of the downstream pipe are presented in Table 5.2. The triple point will not be reached in the safety valve at any of the given heat loads. This is because of the high mass flow rate that will exist at such high heat loads. Reducing the heat load to  $4 \text{ kW/m}^2$  will give a mass flux of  $45 \text{ kg/sm}^2$  and a pressure at the outlet of the safety valve of 4.94 bar which means that dry ice will be formed in the safety relief valve. Increasing the diameter of the downstream pipe will reduce the pressure loss in the downstream pipe. The velocity at the outlet of the downstream pipe at heat loads above  $18 \text{ kw/m}^2$ , corresponding to a mass flux of  $200 \text{ kg/sm}^2$ , is above the maximum velocity according to the standard.

Table 5.2: Pressure loss in downstream pipe

External heat load [ $\text{kW/m}^2$ ]	$\Delta p$ [bar]	G [ $\text{kg/sm}^2$ ]	$u_2$ [m/s]	Ma
5	4.56	56	18	0.08
10	7.74	112	36	0.16
23.5	14.92	264	84	0.38



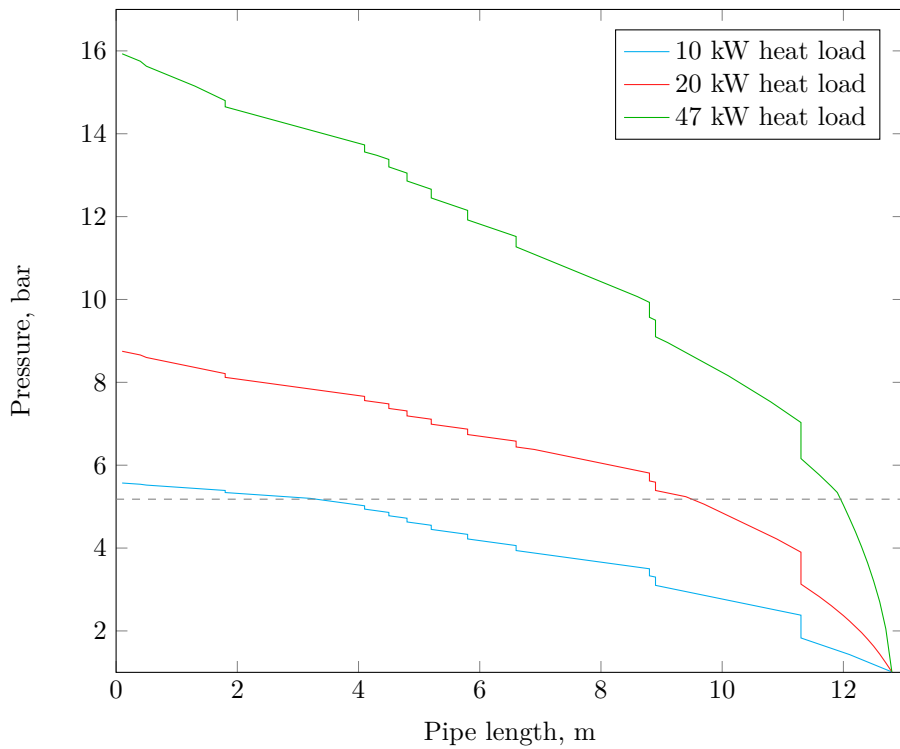


Figure 5.2: Pressure drop per pipe length.

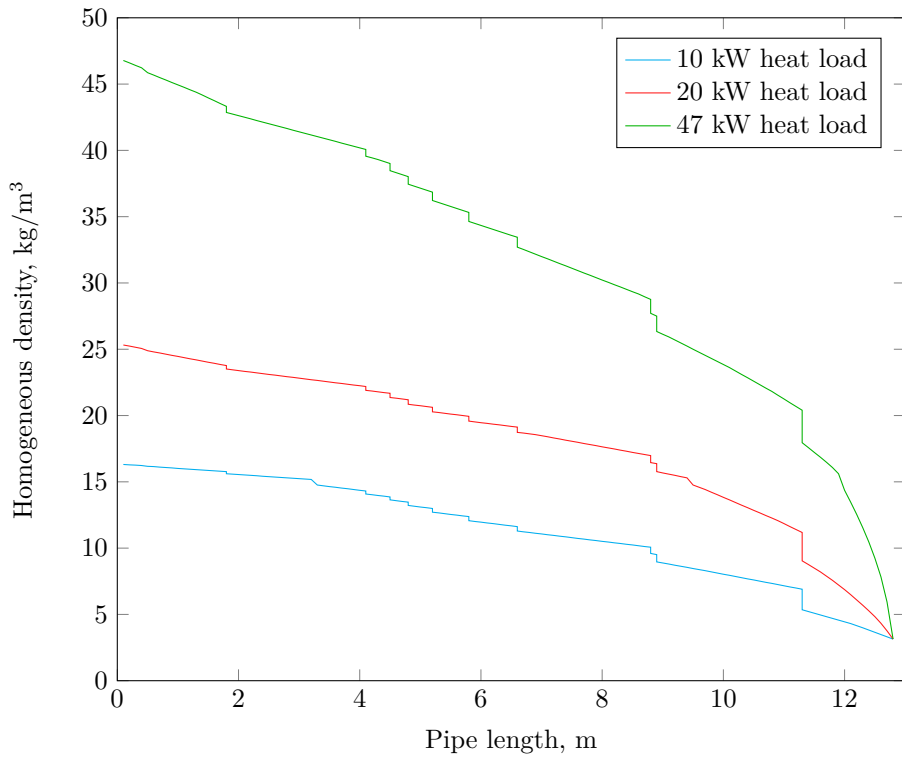


Figure 5.3: Homogeneous density,  $\rho_H$ , per pipe length

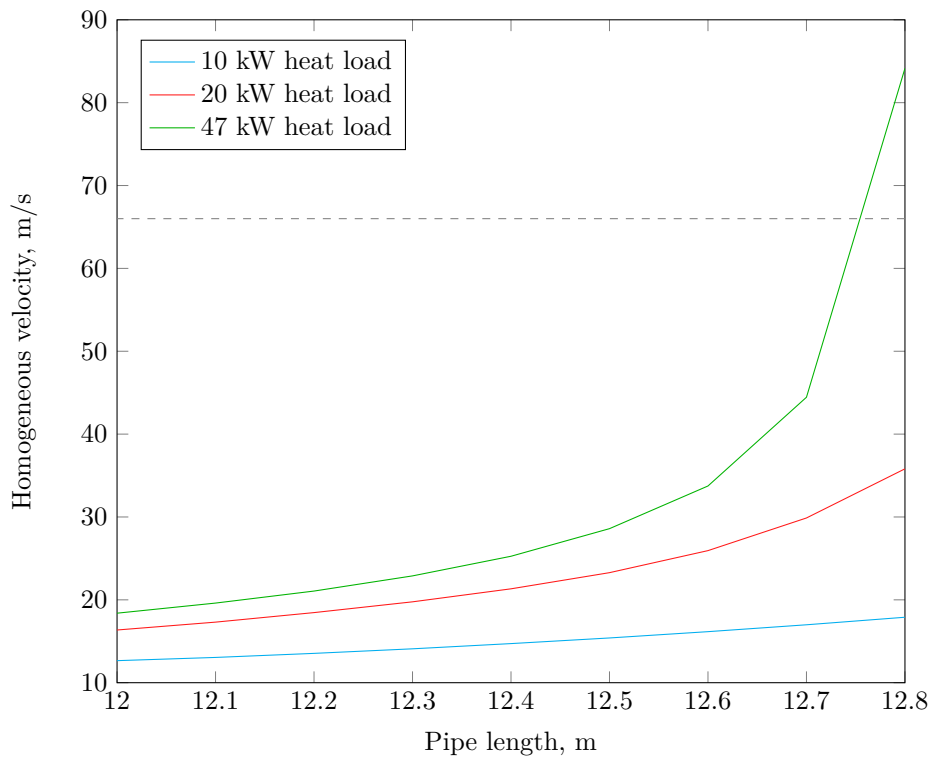


Figure 5.4: Homogeneous velocity,  $u_H$ , per pipe length

## 5.2 Heat transfer

The heat loss to the ambient by free convection as a function of external heat load is presented in Table 5.3. The heat transfer by free convection is not enough to reach the triple point at saturated gas and therefore not enough to avoid formation of dry ice.

Table 5.3: Heat transfer in downstream pipe

Heat load [kW/m <sup>2</sup> ]	$\Delta H^a$ [kW]
5	0.95
10	0.83
23.5	0.64

<sup>a)</sup>ambient temperature 25°C

## 5.3 Pressure drop - EN 13136

The pressure loss based on calculations from NS-EN 13136 is presented in Table 5.4.

Table 5.4: Pressure loss in downstream pipe - EN 13136

	Nuova, d <sub>0</sub> =10mm	Nuova, d <sub>0</sub> =14mm
$\Delta p_{out}$ [bar]	4.92	11.04
$\frac{\Delta p_{out}}{p_0}$	0.07	0.16

The smallest downstream diameter allowed without exceeding 20% of the actual relieving pressure:

- The smallest downstream pipe diameter with Nuova, d<sub>0</sub>=10 mm is 27.2 mm.
- The smallest downstream pipe diameter with Nuova, d<sub>0</sub>=14 mm is 37.0 mm.

Too small pipe diameter may lead to sonic velocity in the downstream pipe and even though the pressure drop is sufficiently low the outlet velocity can become sonic.

The pressure loss in the downstream line for both high pressure safety valves is less than 20 % of the actual relieving pressure ( $p_0$ ). For heat loads of 15 kW/m<sup>2</sup> and lower the velocity at the outlet of the downstream pipe will not reach sonic velocity. The pressure relief system with the downstream line in Figure 5.1 is according to NS-EN 13136 at heat loads up to 15 kW/m<sup>2</sup>.

NS-EN 13136 does not take into account the mass flow rate in the pressure loss calculation unless it is higher than 80 % of the calculated refrigerant mass flow rate

Table 5.5: Outlet velocity

Heat load [kW/m <sup>2</sup> ]	G [kg/sm <sup>2</sup> ]	u <sub>2</sub> <sup>a)</sup> [m/s]	Ma
5	71	22	0.10
10	142	45	0.20
23.5	334	105	0.48

<sup>a)</sup>assuming  $x=0.95$  at outlet

of the pressure relief device.

Table 5.5 shows outlet velocity for a given heat load (mass flow):

According to the standard, the Mach-number should not exceed 0.3 in order to not have critical velocity. This Mach-number is exceeded at a heat load of 15 kW/m<sup>2</sup>.



## Chapter 6

# Discussion

A pressure release system for CO<sub>2</sub> is designed to release CO<sub>2</sub> from a system where the pressure is higher than a predetermined maximum pressure. Precautions has to be taken when designing a pressure release system for CO<sub>2</sub> to avoid formation of solid CO<sub>2</sub> and blockage of the safety valve and downstream pipe.

In Chapter 2 the geometry and upstream flow conditions was investigated to see if it affected the downstream vapor quality. There was a significant difference in the amount of formed dry ice between releasing saturated liquid and saturated gas.

The density of CO<sub>2</sub> is provided by interpolation from Table A.1, see Appendix A. In Chapter 2 the volume-% is calculated based on the density which makes sense and is correct when calculating the homogeneous density, but the actual displaced volume might be larger. As for water there is a difference in density for ice and snow. This difference exists also for carbon dioxide. A video produced by Danfoss [5] shows the formation of dry ice as the pressure reaches the triple point during pressure release and the formed dry ice looks more like snow than ice. This is also verified through pictures from [6]. Dry ice is sold for cooling purposes and Praxair[18] sells solid blocks of dry ice weighting 22.7 kg and having a volume of 0.0142 m<sup>3</sup>, which gives a density of approximately 1599 kg/m<sup>3</sup>. This is compact dry ice displacing no more volume than its own, unlike CO<sub>2</sub> snow where gas exists between the snowflakes.

Advansor releases 10 kg CO<sub>2</sub> within 30 seconds which corresponds to a heat load of 47 kW, but only have 20 kW heat load on the receiver tank. Looking at the video, see Appendix C, the mass flow rate decreases after approximately 10 seconds which makes sense as the heat load is not enough to evaporate the amount of CO<sub>2</sub> liquid that is required to maintain a pressure of 60 bar. The pressure in the receiver tank will drop as a consequence of the negative energy balance. The high pressure safety valve is oversized for its task and releases more CO<sub>2</sub> than what corresponds to the heat load. The results from calculations in this report (with same geometry as Advansor) shows that releasing CO<sub>2</sub> with a mass flow rate corresponding to a heat

load of 47 kW gives sonic velocity in the end of the downstream pipe. Calculations based on the standard also gives sonic velocity in the end of the downstream pipe. This is not according to the standard.

In existing design of pressure relief systems CO<sub>2</sub> is released at saturated gas from a receiver tank. This is to minimize the formation of dry ice when reaching the triple point, illustrated by Figure 2.1. In Chapter 3 different heating systems were discussed to avoid formation of dry ice and calculations were done and presented in Chapter 5. The results showed that for ambient temperature of 25°C and with the assumptions that the downstream pipe has the same surface temperature as the flow the heat transfer due to free convection from ambient air to the downstream pipe was less than 1 kW. In order to avoid dry ice by heat transfer by free convection the ambient temperature has to be above 200°C. At such high temperature the systems equipment might be exposed to damage by the high temperature rather than dry ice blockage.

A bypass solution with multi-stage heating seems like the most favorable solution for heating of the downstream flow. The safety valve releases CO<sub>2</sub> to a bypass pressure at for example 7 bar at which the flow is exposed to an external heat source like a heat membrane on the pipe wall. At the same time the flow is lead away to a safe place, for example the roof of a building, where another pressure relief valve releases the flow, that after heating is superheated gas, to atmospheric pressure.

The simulation of the pressure development through the downstream pipe shows a significantly increase in velocity towards the end. This is because the density decreases as the pressure reaches the atmospheric pressure. The increasing flow velocity will lead to increasing frictional pressure loss through the downstream pipe. As a result of decreasing density the pressure loss is increasing significantly towards the end of the downstream pipe.

The flow in the downstream line shall not reach critical speed (sonic velocity), which by [21] is defined as  $Ma > 0.3$ . Calculation using NS-EN 13136 and a heat load of 30 kW/m<sup>2</sup> gives an outlet velocity of 134 m/s which corresponds to a Mach number of 0.60. The speed of sound for CO<sub>2</sub> gas at 1 atm and -78°C is 220 m/s. That means that the maximum velocity in the downstream pipe is 66 m/s which gives a maximum allowed heat load is 15 kW/m<sup>2</sup>. The calculations based on Martinelli-Nelsons equation for two-phase frictional pressure drop having a heat load of 30 kW/m<sup>2</sup> gives an outlet velocity of 107 m/s which corresponds to a Mach number of 0.49. For this calculation the maximum allowed heat load is 18 kW/m<sup>2</sup>.

A solution to avoid the high velocity is to replace the end of the downstream pipe by a tapered channel. Yamaguchi [22] concluded that deposition of dry ice was greatly eased when using tapered channel instead of sudden expansion. By increasing the flow area the velocity is decreased and sonic velocity can be avoided. The decrease in density is compensated with a larger flow area. On the other hand the pressure loss will be less as the pipe diameter increases, which means the triple point will be reached earlier in the downstream pipe.



From Figure 5.2 it can be seen that for external heat loads above 10 kW the triple point is reached in the downstream line and not in the safety valve. Another interesting observation is that for heat load above 40 kW the triple point is reached after the last bend in the downstream pipe. This reduces the possibility for blockage significantly. On the other hand, increasing the heat load leads to higher mass flow rate which means possibilities of sonic velocity in the downstream pipe.



# Chapter 7

## Experimental setup

Experimental work can be done to investigate further how carbon dioxide behave during pressure release. The previously work done in this report is only based on empirical correlations and have probably a significant amount of error. This chapter contains a simple overview of what is needed to do a practical experiment with pressure release of carbon dioxide. Unfortunately there was no opportunity to implement an experimental test program for investigation of the function of pressure relief valves and downstream pipe systems.

### 7.1 Experiments

A test program should include investigation and evaluation of the function of a pressure relief system under conditions relevant for the refrigeration industry with emphasis on supermarket refrigeration. In the refrigeration industry both pressurized liquid and pressurized gas may have to be vented to the atmosphere in case of an emergency or for maintenance. The pressure relief systems used in the refrigeration industry today consist of safety relief valves, often dimensioned for higher mass-flow rates than required [1], and downstream pipes that leads the carbon dioxide to a safe place (usually outdoor).

A test setup for pressure release of carbon dioxide requires equipments. Pressurized carbon dioxide, both liquid and gaseous, are needed.  $\text{CO}_2$  is released from a receiver tank. The amount of carbon dioxide needs to meet the requirement of a given external heat load for a given time. A heat load of 20 kW gives a mass flow rate of 0.14 kg/s at pressure release of saturated gas at 60 bar. Increasing the heat load will increase the mass flow rate as long as it doesn't exceeds the maximum flow rate through the safety release valve. Increasing the mass flow rate without increasing the heat load will lead to a drop in pressure in the receiver tank. Heat load on the tank can be obtained by hot water in an internal coil.

A safety valve should be placed at the top of the receiver tank in order to release saturated gas. In case of pressure release for safety reasons the safety valve will open when the pressure in the receiver tank exceeds the set pressure. In case of emptying the receiver tank a release valve is opened until the pressure in the receiver tank is equal to the atmospheric pressure. When emptying a receiver tank containing CO<sub>2</sub> there is a possibility that some dry ice will be formed as the triple point is reached, and this dry ice will not be released through the safety valve as it accumulate at the bottom of the receiver tank.

Suggestion for experimental work:

- Closer look at the pressure development through the last part of the downstream pipe where the velocity is increasing significantly.
- Investigate the influence of replacing the last part of the downstream pipe with a tapered channel.
- Test the concept of multi-stage heating / by-pass release with two pressure relief valves.
- Investigate the pressure development through different downstream pipe systems used in the refrigeration industry. Vary the mass flow, pipe length, pipe diameter and number of bends.
- Empty the receiver tank and see how much dry ice that is left, and how much the pressure will rise after closing the release valve.

## Chapter 8

# Conclusion

To avoid possible hazardous situations from pressure release of CO<sub>2</sub>, CO<sub>2</sub> should be heated to superheated gas before it is released to atmospheric pressure. Then no dry ice will be formed. If that is not possible care should be taken when designing the downstream pipe system. The pressure loss in a downstream pipe increases with increasing mass flux. The outlet flow velocity also increases with increasing mass flux. A significant part of the pressure loss is taking place in the end of the downstream pipe because of the increase in flow velocity. It means that for high mass fluxes (100-200 kg/sm<sup>2</sup>) the triple point can be reached in the last part of a sufficient long downstream line, without having sonic velocity at the outlet or exceed the maximum pressure according to the standard ( $\Delta p_1 < 20\%$  of  $p_0$ ). A safety release valve should be as efficient as possible. In order to avoid dry ice formation in the safety release valve and blockage of the downstream pipe when releasing CO<sub>2</sub> from saturated gas the mass flux should be as high as possible without causing sonic flow velocity at the outlet.



# Bibliography

- [1] Advansor, 2014. Testing for frost formation in exhaust pipes when releasing safetyvalve, written report from test of releasing carbon dioxide, with two short videos.
- [2] AGA Rommenhöller - Ideen and Gase, 1989. Eigenschaften der kohlendioxid, 11–11.
- [3] Chisholm, D., 1980. Two-phase flow in bends. *Int. J. Multiphase Flow* 6, 363–367.
- [4] Churchill, S. W., Chu, H. H. S., 1975. *Int. J. Heat Mass Transfer* 18, 1049.
- [5] Danfoss, November 2011. CO<sub>2</sub> phase changes.  
URL <https://www.youtube.com/watch?v=SkSkKK1cVJQ>
- [6] Dongping, H., 2006. Experimental investigation and theoretical analysis of blockage in CO<sub>2</sub> safety valves and their downstream pipes. Ph.D. thesis, Shanghai Jiao Tong University.
- [7] Dongping, H., Quack, H., Ding, G., 2007. Experimental study of throttling of carbon dioxide refrigerant to atmospheric pressure. *Applied Thermal Engineering* 27, 191–192.
- [8] European Committee for Standardization, 2013. Refrigeration systems and heat pumps - pressure relief devices and their associated piping - methods for calculation, ns-en 13136. Tech. rep., European Committee for Standardization.
- [9] Haukås, H. T., 2005. Kulde- og varmeprosesser med CO<sub>2</sub> som kuldemedium.
- [10] Incropera, F. P., DeWitt, D. P., Bergman, T. L., Lavine, A. S., 2006. *Fundamentals of Heat and Mass Transfer*. John Wiley & Sons.
- [11] Lockhart, R. W., Martinelli, R. C., 1947. Proposed correlation of data for isothermally two-phase, two-component flow in pipes. *Chemical Engineering Progress* 45, 39–48.
- [12] Lorentzen, G., 1994. Revival of carbon dioxide as a refrigerant. *International Journal of Refrigeration* 17, 292–301.

- [13] Martinelli, R. C., Nelson, B., 1948. Prediction of pressure drop during forced-circulation boiling water. Transactions ASME 70, 695–702.
- [14] Moran, M. J., Shapiro, H. N., 2006. Fundamentals of Engineering Thermodynamics. John Wiley & Sons.
- [15] Morgan, V. T., 1975. The overall convective heat transfer from smooth circular cylinders. Advances in Heat Transfer 11, 199–264.
- [16] Nuova General Instruments, February 2015. High pressure safety valves.  
URL <http://www.nuovageneral.it/index/en/prodotti/high-pressure-safety-valves.html>
- [17] Ozone Secretariat United Nations Environment Programme, 2000. The montreal protocol on substances that deplete the ozone layer. The Montreal Protocol on Substances that Deplete the Ozone Layer.
- [18] Praxair, February 2015. Carbon dioxide, safety data sheet.  
URL <http://www.praxair.com/~media/North%20America/US/Documents/SDS/Dry%20Ice%20UltraIce%20CO2%20Safety%20Data%20Sheet%20SDS%20P4575.pdf>
- [19] Skaugen, G., 2011. A short memo on how to extend the uv formulation to vapour-solid phase.
- [20] Stiftelsen Returgass, Januar 2015. Beregningsprogram.  
URL <http://www.returgass.no/Hovedmeny/Tjenester/Beregningsprogram.aspx>
- [21] White, F. M., 2008. Fluid Mechanics. McGraw-Hill.
- [22] Yamaguchi, H., Iwamoto, Y., Ozaki, S., Nekså, P., 2014. Experimental observation of sedimentation phenomena of CO<sub>2</sub> dry ice in model channel. 11<sup>th</sup> IIR Gustav Lorwntzen Conference on Natural Refrigerants, Hangzhou, China.



# Appendices



# Appendix A

## Thermodynamic data

### A.1 Thermophysical properties of CO<sub>2</sub>

Above the triple point thermodynamic data are provided by rnlb, see [20]. Rnlb is integrated in Microsoft Excel.

Below the triple point thermodynamic data are provided based on Table A.1, which is taken from [2] and [19]. Interpolation between the points is done to get hundredth value of pressure, which is necessary for simulation.

Values for specific enthalpy and specific entropy from the table are adjusted to fit with the given data in rnlb, which has another reference state.

Table A.1: Thermodynamic properties of CO<sub>2</sub>

T °C	T [K]	P [bar]	$\rho_s$ [kg/m <sup>3</sup> ]	$\rho_g$ [kg/m <sup>3</sup> ]	$h_s$ [kJ/kg]	$h_g$ [kJ/kg]	$s_s$ [kJ/kgK]	$s_g$ [kJ/kgK]
-56.6	216.55	5.18	1512.4	13.84	105.55	649.33	2.8156	5.3273
-60	213.15	4.1	1521.9	10.97	99.27	649.21	2.7863	5.3671
-65	208.15	2.87	1534.6	7.74	89.97	648.41	2.7428	5.4261
-70	203.15	1.98	1546.1	5.29	82.02	646.94	2.7043	5.4860
-75	198.15	1.34	1556.5	3.71	75.07	645.02	2.6695	5.5467
-78.9	194.25	0.98	1564	2.74	70.05	643.18	2.6345	5.5948

### A.2 Thermophysical properties of air

The data in Table A.2 are found in Fundamentals of Heat and Mass Transfer, [10]. The table is interpolated to get values for each whole degree.

Table A.2: Thermodynamic properties of air at atmospheric pressure

T K	T [°C]	$\nu \cdot 10^7$ [m <sup>2</sup> /s]	$k \cdot 10^3$ [W/mK]	$\alpha \cdot 10^6$ [m <sup>2</sup> /s]	Pr [-]
200	-73	7.59	18.1	10.3	0.737
250	-23	11.44	22.3	15.9	0.720
300	27	15.89	26.3	22.5	0.707
350	77	20.92	30.0	29.9	0.700
400	127	26.41	33.8	38.3	0.690
450	177	32.39	37.3	47.2	0.686
500	227	38.79	40.7	56.7	0.684
550	277	45.57	43.9	66.7	0.683
600	327	52.69	46.9	76.9	0.685
650	377	60.21	49.7	87.3	0.690
700	427	68.10	52.4	98.0	0.695
750	477	76.37	54.9	109	0.702
800	527	84.93	57.3	120	0.709
850	577	93.80	59.6	131	0.716
900	627	102.9	62.0	143	0.720
950	677	112.2	64.3	155	0.723
1000	727	121.9	66.7	168	0.726

# Appendix B

## Ts-diagram

Figure B.1 shows a temperature-entropy phase-diagram of  $\text{CO}_2$ .

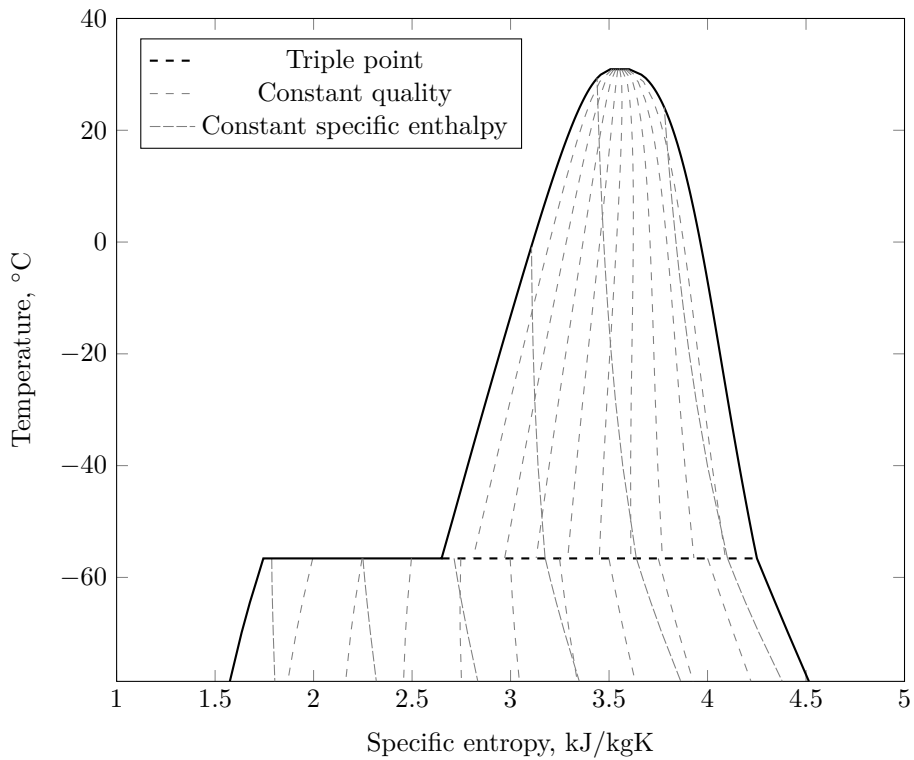


Figure B.1: Temperature-Entropy diagram of  $\text{CO}_2$



# Appendix C

## Screenshots

Figure C.1 shows the downstream pipe direct after the safety valve is opened.



Figure C.1: Screenshot from video by Advansor.

Figure C.2 shows the downstream pipe 10 seconds after the safety valve is opened.

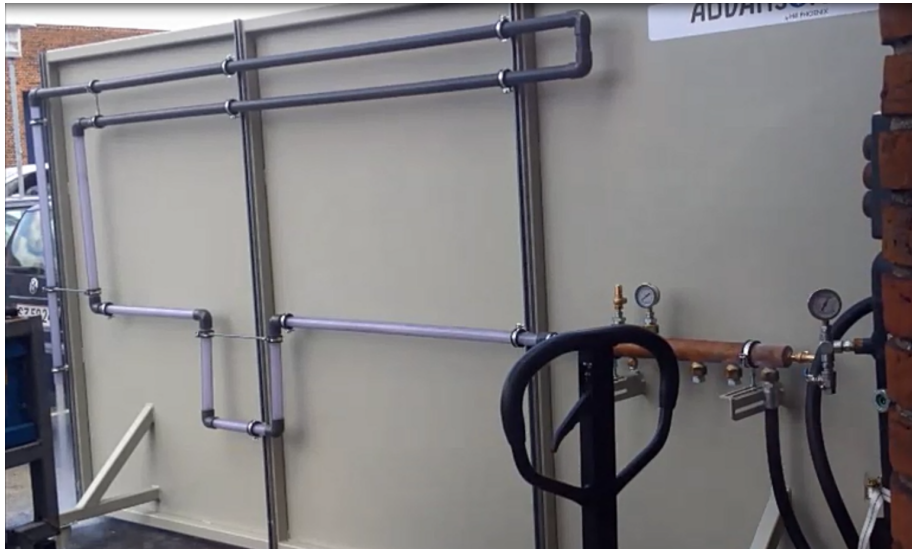


Figure C.2: Screenshot from video by Advansor.